

N83 22306

D17

VEHICLE CHARGING AND POTENTIAL ON THE STS-3 MISSION

Roger Williamson
Stanford University

Preceding page blank

VEHICLE CHARGING AND POTENTIAL ON THE STS-3 MISSION

P.R. Williamson and P.M. Banks
STAR Laboratory/SEL, Stanford University, Stanford, CA 94305

W.J. Raitt
Center for Atmospheric and Space Science
Utah State University, Logan, UT 84322

**ORIGINAL PAGE IS
OF POOR QUALITY**

The Vehicle Charging And Potential (VCAP) experiment flown on the STS-3 mission was designed to study the electrical interaction of the shuttle orbiter with the low earth orbit environment. The interaction of a large, orbiting body with the low earth space environment is not well known. With the initiation of an operational era in space, it is necessary that we understand (1) the perturbations produced by the orbiter as it moves through the near earth environment, (2) the environment as provided to instrumentation operating in the payload bay of the orbiter and (3) the effects that the environment exerts upon the orbiter itself. Future missions which depend upon knowledge of the electrical interaction of the orbiter with the space environment include those with high power charged particle beam experiments and others with long antennas operating at high voltages in the VLF frequency range. Also, when operations begin with orbit inclinations above about 50 degrees, large fluxes of energetic electrons (and protons) will bombard the orbiter when the vehicle is at high magnetic latitudes. In the past, satellites have been adversely affected by electrical discharges induced by energetic particle bombardment and these problems present similar concerns for the dielectric covered orbiter. The VCAP experiment on STS-3 was designed to study the interactions between the orbiter and the environment which are of importance to understanding these problems.

INSTRUMENTATION

An electron gun with fast pulse capability was used in the VCAP experiment to actively perturb the vehicle potential in order to study dielectric charging, return current mechanisms and the techniques required to manage the electrical charging of the orbiter. Return currents and charging of the dielectrics were measured during electron beam emission and plasma characteristics in the payload bay were determined in the absence of electron beam emission.

The VCAP instrumentation as flown on the OSS-1 pallet during STS-3 includes five separate pieces of hardware:

1. Fast Pulse Electron Generator (FPEG) - The FPEG (Figure 1) consists of two independent electron guns which are of the diode configuration with a directly heated tungsten filament and a

Preceding page blank

tantalum anode. The two guns, designated as FPEG 1 AND FPEG 2 emit electrons with an energy of 1000 eV at currents of 100 mA and 50 mA, respectively. The electron beams are collimated to a beam width of about 5 degrees by focus coils mounted just beyond the anodes. Each gun is controlled by a 37 bit serial command word which selects the gun to be used, controls filament and high voltage power supplies, determines the on time, off time and number of pulses of the beam. The times are controllable in 32 logarithmic steps from 600 nanoseconds to 107 seconds and the number of pulses is controllable in powers of two from 1 to 32,768. The rise and fall times for the electron beam are 100 nanoseconds so that very short pulses (and therefore small increments of charge) can be emitted.

2. Charge Current Probes (CCP1 and CCP2) - Each Charge Current Probe (CCP) consists of two adjacent sensors --- one metallic and one dielectric --- as shown in Figure 2. The current flowing to the metallic sensor is used as an indication of the return current to exposed metal surfaces on the orbiter. The dielectric sensor provides a measurement of the charge accumulation on dielectric surfaces of the orbiter, the material used for the charge probe dielectric is from the same batch of Flexible Reusable Surface Insulation (FRSI) that was used on the Columbia (OV-102) and covers the payload bay doors and upper wing surfaces (Figure 3). Both of the CCP sensors respond to changes in the orbiter potential with rapid time response. Measurement rates were set at 60 samples per second but peak hold measurements of both current and charge were made which allowed spikes longer than 100 nanoseconds to be captured.

The Charge Probe measures directly the charging of a piece of FRSI. Since this is the same material as covers the payload bay doors and upper wing surfaces, we assume that measurements made on the FRSI in the payload bay are indicative of the behavior of this same material on the orbiter. The FRSI material on the Charge Probe covers an isolated metal plate which is connected to the input of a charge amplifier (Figure 4). When a charge is induced on the surface of the dielectric a similar (but opposite) amount of charge is induced on the metal plate. The charge amplifier converts the charge to a voltage which is the source of the data shown for the CCP measurement of vehicle potential. If the vehicle potential changes and the surrounding plasma provides a current to charge the surface of the dielectric, then the potential measured by the Charge Probe is an accurate measurement of the vehicle potential. If an electric field exists at the surface of the FRSI, then the measured potential is less than the actual vehicle potential.

Two sets of the CCP (designated CCP1 and CCP2) were used with CCP1 mounted adjacent to the FPEG and CCP2 mounted on the opposite corner of the pallet as far away from the FPEG as possible. These probes provide measurements of vehicle potential changes and return currents induced by operation of the FPEG with high time resolution at voltages up to 1000 volts and currents up to 4 mA.

3. Spherical Retarding Potential Analyzer (SRPA) - The Spherical Retarding Potential Analyzer (Figure 5) measures the density and energy of ions and provides an absolute value for the vehicle potential as well as a measurement of the plasma environment in the payload bay. The SRPA has a 19 cm diameter spherical collector surrounded by a 20 cm diameter spherical grid. The biasing voltages applied to these electrodes result in the collection of positive ions by the collector. In the frame of reference of the orbiter the dominant ambient ion O^+ will have a drift energy of approximately 5 eV. This energy is related to the orbiter velocity, which is well known, so any deviation of the O^+ drift energy from the expected value gives a measure of the electrical potential of the orbiter structure relative to the ionosphere. A Langmuir probe is attached to the SRPA. This probe is a small, spherical probe which measures the density and temperature of electrons and provides a cross check on the vehicle potential. The SRPA/Langmuir probe instrument is mounted on a corner of the pallet as far from other surfaces as possible to give the best opportunity to acquire data uncontaminated by wake effects.
4. Digital Control Interface Unit (DCIU) - The Digital Control Interface Unit provided all signal, command and power interfaces between the VCAP instrument and the pallet. Power switching and command decoding were done in the DCIU. Three microprocessors (1802 type) were used in the DCIU. The control microprocessor stored sequences of time-tagged serial commands in both ROM and RAM. These sequences of commands could be initiated in response to a single command sent from a source external to the DCIU and perform a series of operations such as FPEG pulsing, gain changing and resets. A second microprocessor was used to control the offset of the SRPA sweep voltage. The third microprocessor was used to monitor temperatures, voltages and currents and to set out of limit flags passed as bi-level signals to the orbiter GPC for display and alarm signaling.

Placement of the instrumentation on the OSS-1 pallet is shown in Figure 6. The SRPA (and Langmuir probe) is on one corner of the pallet (far left in the figure). The CCP's occupy positions on two opposite corners of the pallet, one on the lower right in the figure and the other partially hidden at the top of the figure. The electron gun (FPEG) is adjacent to the CCP at the lower right and is shown with a circular gun head.

MEASUREMENTS

Passive and active operations were performed during OSS-1. The SRPA and CCP's were operating throughout the mission and data obtained when the electron gun was not being operated determine the characteristics of the orbiter and the payload bay environment in the absence of perturbations from active experiments.

ORIGINAL PAGE IS
OF POOR QUALITY

SRPA data taken in passive mode with the payload bay in the ram direction (the direction of the velocity vector) are shown in Figures 7 and 8. In the daytime (Fig. 7) the SRPA signal is relatively high as compared to the expected ambient measurement and does not show the peak at energies around 5 volts where the peak signal associated with the atomic oxygen ion should be. The Langmuir probe data show that the vehicle potential is offset by about 0.5 volt from the ambient plasma at the location of the SRPA. At night (Fig. 8) the measurements are much lower and in some cases the O^+ peak of atomic oxygen ions can be seen. The shift in the peak of the O^+ ions and the shift in the Langmuir probe sweep indicate that the vehicle potential has been shifted by about 1 volt.

As the orbiter rolls very strong ram/wake effects are observed on plasma in the vicinity of the payload bay. Averages of the SRPA and Langmuir probe data are shown in Figure 9 and show this dramatic variation. The SRPA ion current is shown in two different channels called IPL and IPH for ion probe low and ion probe high. These channels are two different range measurements of the same signal. The Langmuir probe current is shown in the LP data and represents the density of electrons. In the PTC mode the orbiter rolls about the X axis at 0.4 degrees per second. As the payload bay alternates between the ram direction and the wake of the vehicle, the ion and electron currents alternate between high and low values. In the daytime the SRPA IPL channel saturates. When the orbiter is in shadow the most sensitive channel of the SRPA (IPH) shows no measurable signal. The measurements from the Langmuir probe are less sensitive but show similar behavior.

Measurements of the vehicle potential offset indicate that the main engine nozzles provide a reference potential to the ionospheric plasma surrounding the vehicle. Because the orbiter is 97% covered with dielectric materials, the main engine nozzles provide the primary contact between the orbiter metallic structure and the plasma. The velocity of the vehicle relative to the surrounding plasma induces a potential difference between any location on the orbiter and the main engine nozzles. The Langmuir probe measures this potential difference which is shown in Figure 10A for one orbit. The computed potential is shown in Figure 10B assuming that the main engine nozzles provide the reference point for the potential. The variation in the potential is caused primarily by the changing relative attitude of the orbiter with respect to the velocity vector and the direction of the geomagnetic field. Because the orbiter is so large and the nozzles form the voltage reference point, this variable voltage offset (which amounts to about 200 mV per meter of distance between the nozzles and the measurement point) must always be taken into consideration in the operation of any plasma diagnostic instrument which is sensitive to errors on the order of a few volts.

Active experiments were performed by emitting a series of electron beam pulses. Data taken during one such sequence, designed to study vehicle charging and return current mechanisms and labeled Charge Current (CC), is shown in Figure 11. Each pulse group consists of 16 pulses of increasing width. The sequence begins with one microsecond pulses (which show no measurable perturbation.) When the pulse widths are increased to more than a millisecond in duration significant charging of the orbiter occurs with induced potentials of tens of volts. The potentials measured close to the FPEG are higher than those on the far side of the pallet and

may indicate that a sheath developed around the vehicle. The currents at the two locations (CCP1 and CCP2) are also different with the larger current near the electron gun as might be expected since the beam produces locally enhanced ionization levels.

A higher time resolution plot of a portion of the same CC sequence is shown in Figure 12. The currents measured recover to their normal non-emission levels in the short time between pulses, but the charge on the dielectric is retained and decays much more slowly. Time constants for the vehicle potential (or dielectric charging) to return to non-emission levels vary from less than one second up to minutes. An example of the slow decay of the dielectric charge can be seen at 0423:45 GMT in the Charge 2 data.

CONCLUSIONS

The VCAP experiment on STS-3 has shown that active, controlled experiments can be successfully performed from the payload bay of the orbiter. Electron beams have been used to perform a series of experiments to study the electrical interaction of the orbiter with the surrounding environment and the environment provided to the payload. The emi levels during the mission were the lowest experienced during the project and were unmeasurably low on orbit. The thrusters produced disturbances which were variable in character and magnitude. Strong ram/wake effects were seen in the ion densities in the payload bay. Vehicle potentials are variable with respect to the plasma and depend upon location on the vehicle relative to the main engine nozzles, the vehicle attitude and the direction of the geomagnetic field.

Acknowledgements

This work was conducted with support under NASA contract NAS5-24455 at Utah State University and Stanford University and by NASA grant NAGW 235 at Stanford University. Many people have contributed to this project over the last five years and we especially wish to acknowledge the contributions of Mr. A.B. White at Utah State University. Special thanks are extended to Dr. O.K. Garriott at Johnson Space Center for his aid, particularly in organizing the Photo/TV observations. The VCAP experiment could not have been done without the careful attention and extensive participation of the flight crew, Cols. Jack Lousma and Gordon Fullerton.

ORIGINAL PAGE IS
OF POOR QUALITY

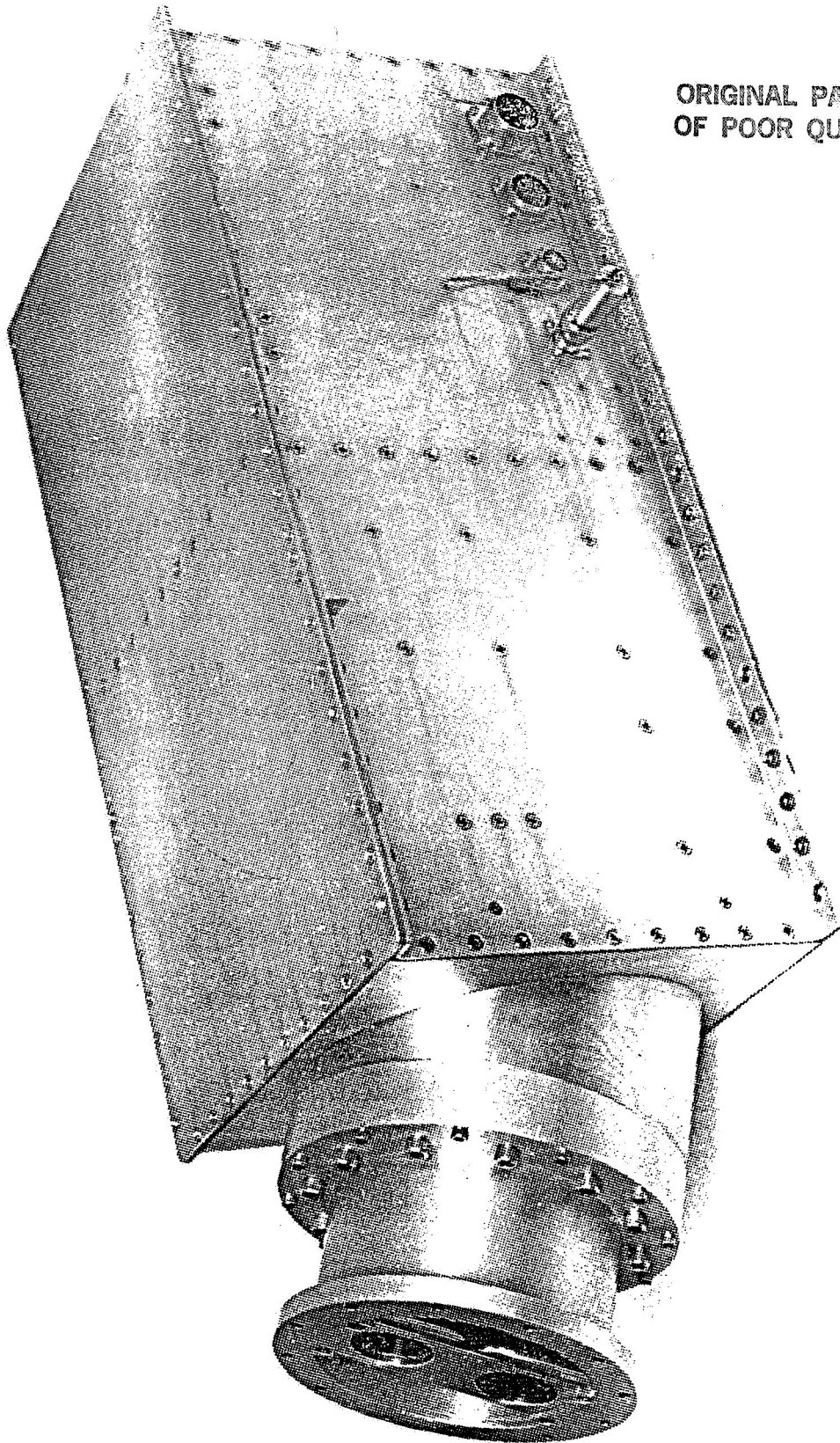


Figure 1. Photograph of the fast pulse electron generator. The two ports through which the electron beams are emitted can be seen at the left of the unit. The mated connector at the right of the unit is an arming plug which is removed during integration to avoid accidental heating of the filaments.

ORIGINAL PAGE IS
OF POOR QUALITY

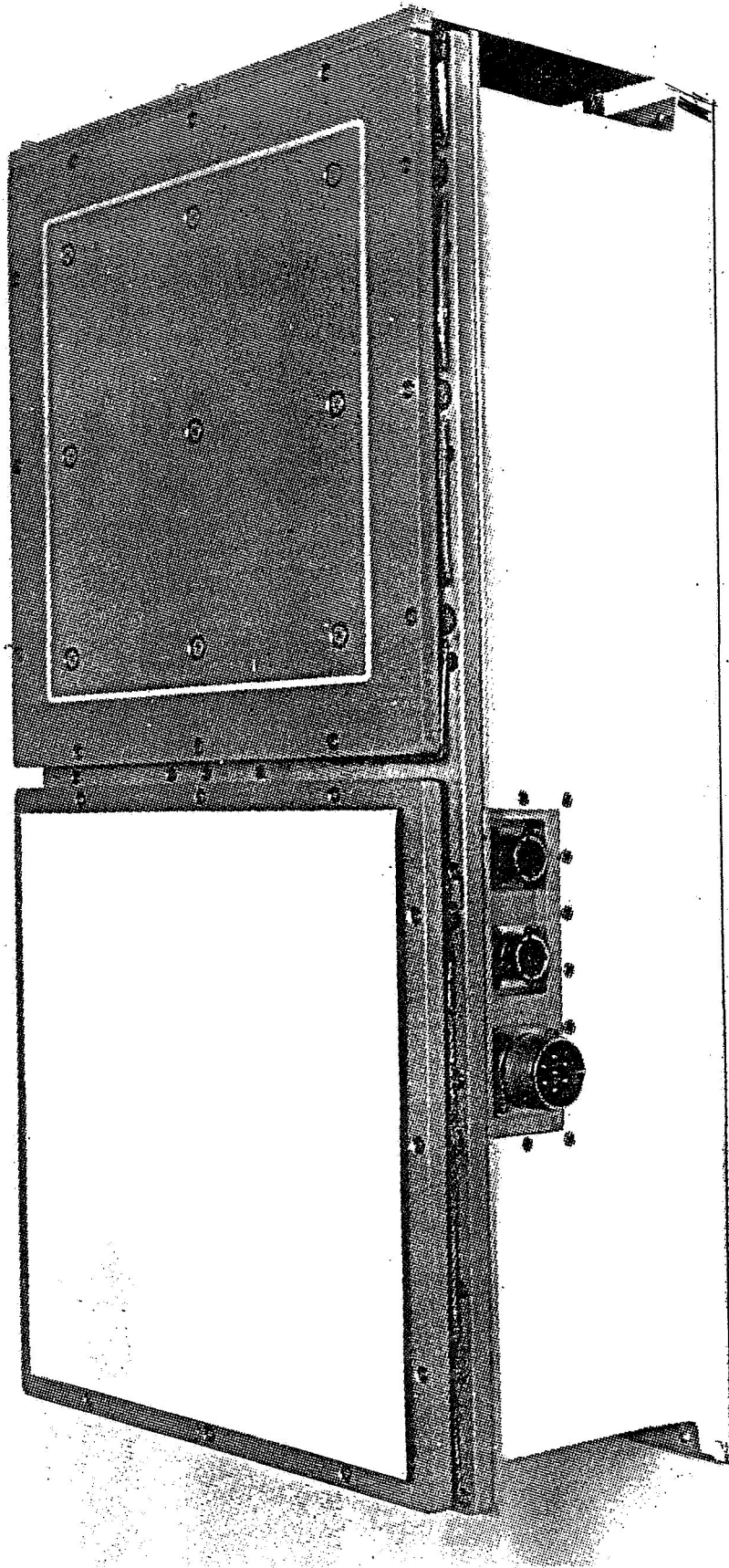
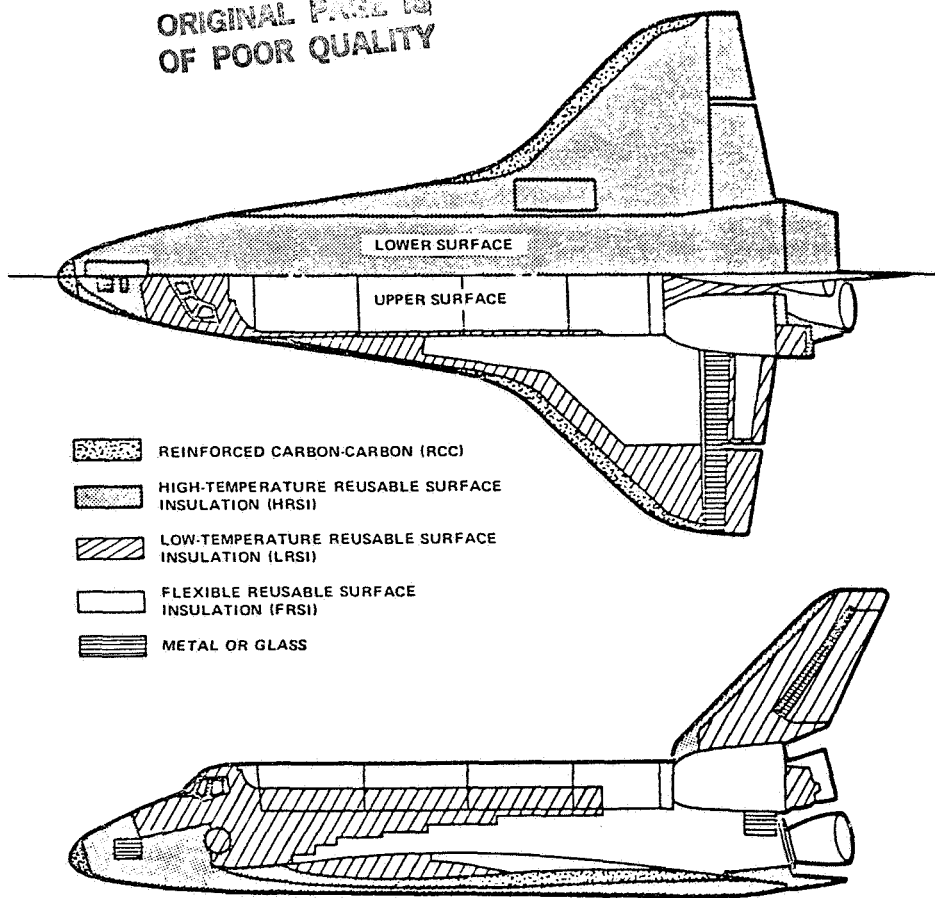


Figure 2. Photograph of one of the charge and current probes. The light colored surface to the left is the FRSI charge collecting surface, while the darker surface to the right is a gold-plated current collector.

ORIGINAL PAGE IS
OF POOR QUALITY



Insulation	Temperature limits	Area, m ² (ft ²)	Weight, kg (lb)
Flexible reusable surface insulation	Below 644 K (371° C or 700° F)	319 (3 436)	499 (1 099)
Low-temperature reusable surface insulation	644 to 922 K (371° to 649° C or 700° to 1200° F)	268 (2 881)	917 (2 022)
High-temperature reusable surface insulation	922 to 978 K (649° to 704° C or 1200° to 1300° F)	477 (5 134)	3826 (8 434)
Reinforced carbon-carbon	Above 1533 K (1260° C or 2300° F)	38 (409)	1371 (3 023)
Miscellaneous			632 (1 394)
Total		1102 (11 860)	7245 (15 972)

Figure 3. Thermal Protection System (TPS) on the orbiter which is about 97% covered with dielectric materials.

ORIGINAL PAGE IS
OF POOR QUALITY

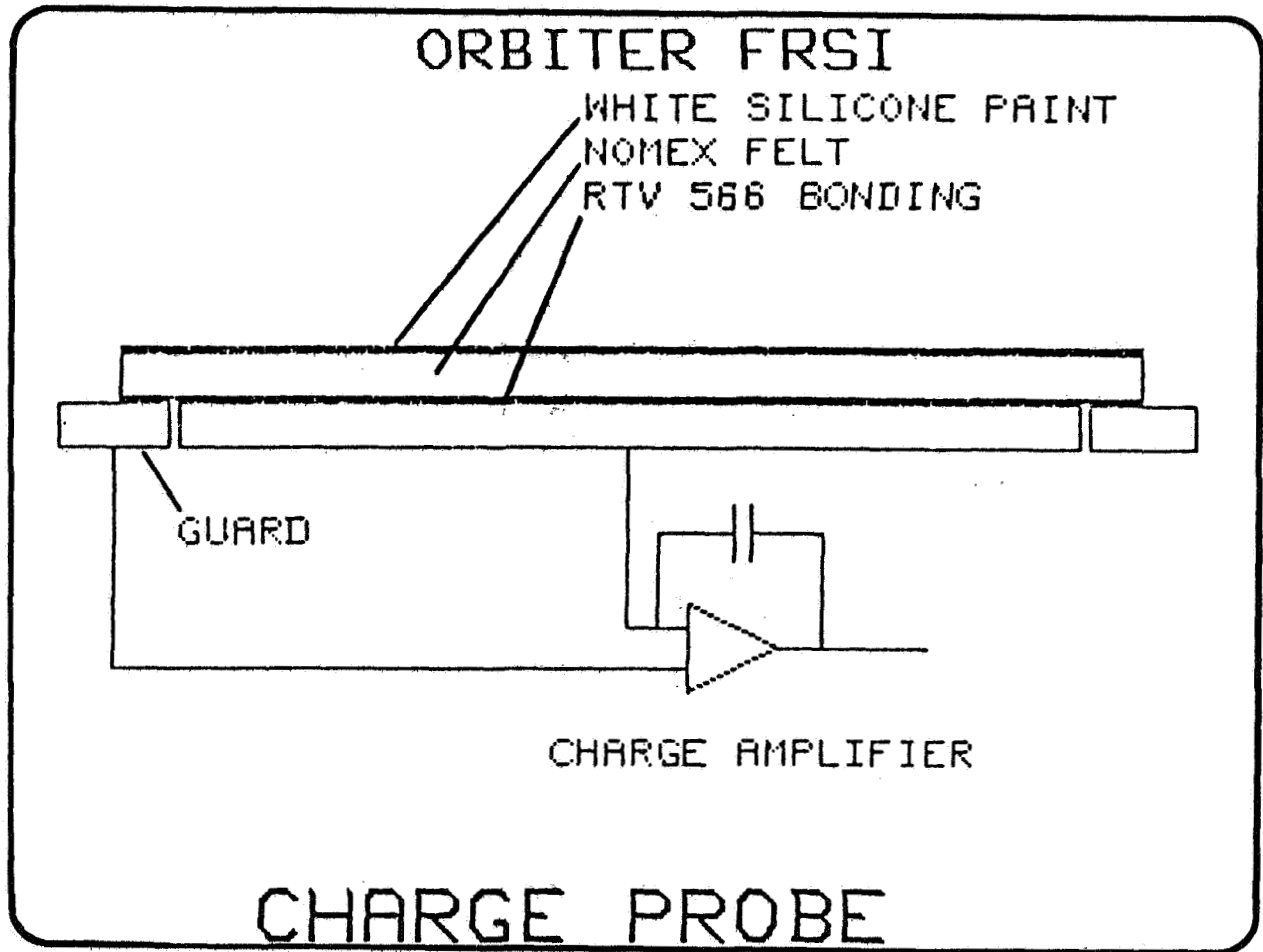


Figure 4. Charge Probe sensor plate construction and the input charge amplifier.

ORIGINAL PAGE IS
OF POOR QUALITY

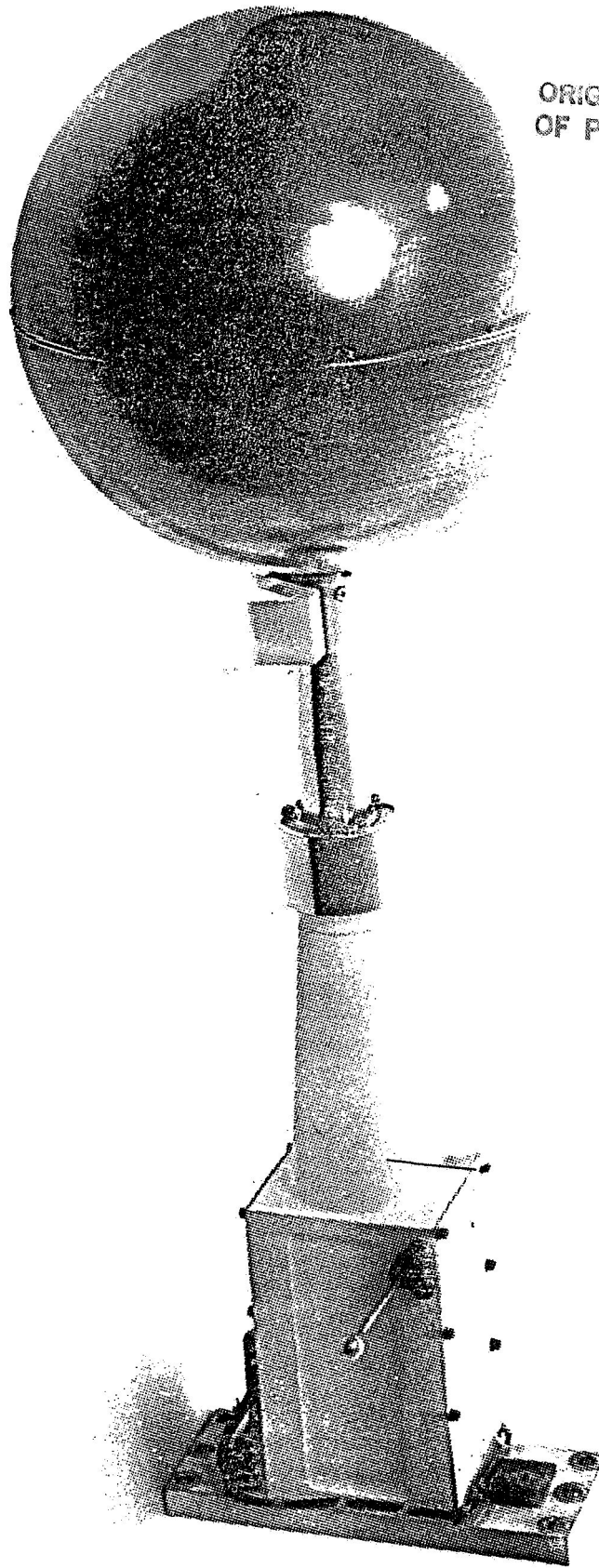


Figure 5. Photograph of the spherical retarding potential analyzer and Langmuir probe assembly. The rectangular box to the right houses preamplifier for the probe signals and is coated with a conducting paint to meet both thermal control and electrical requirements.

ORIGINAL PAGE IS
OF POOR QUALITY

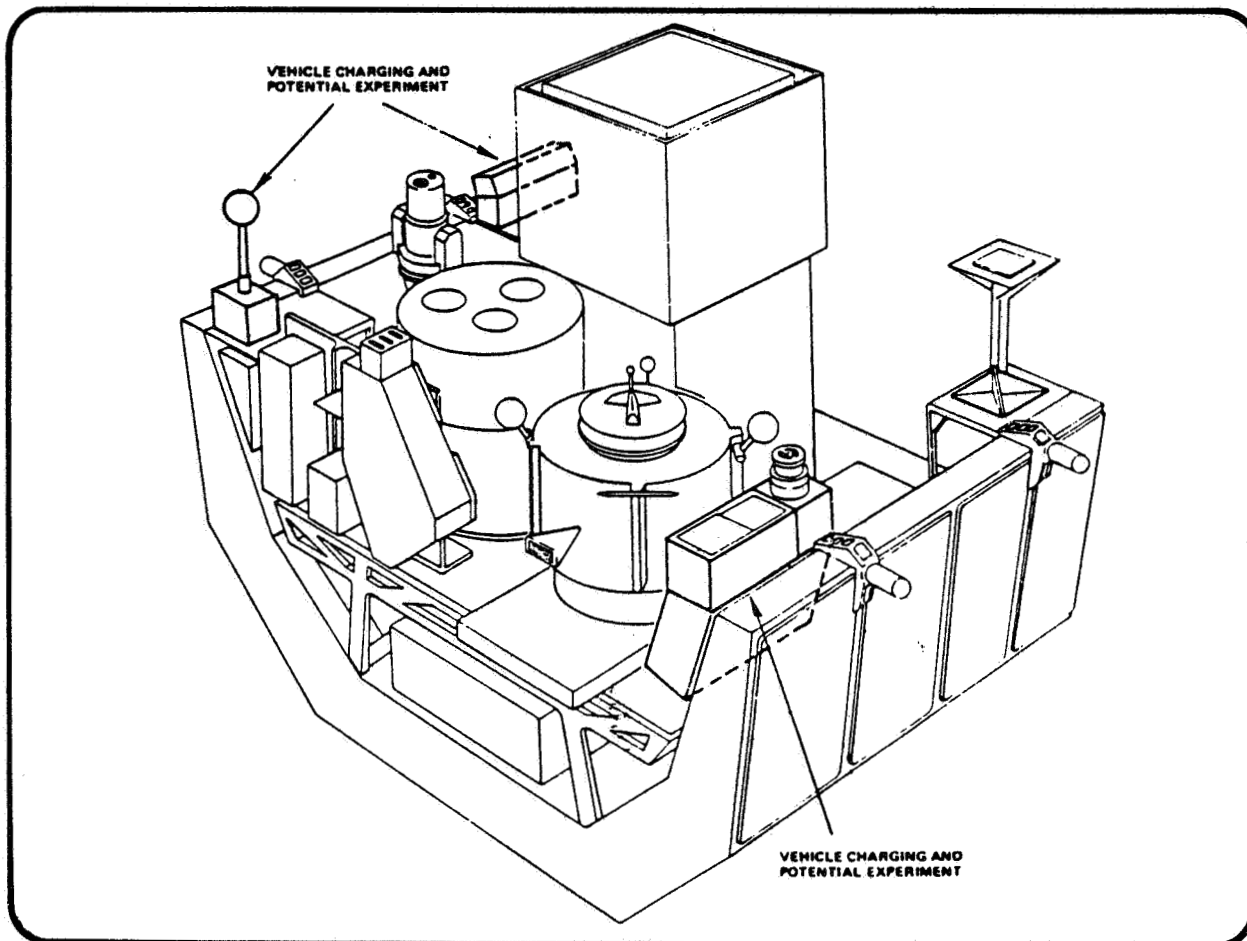
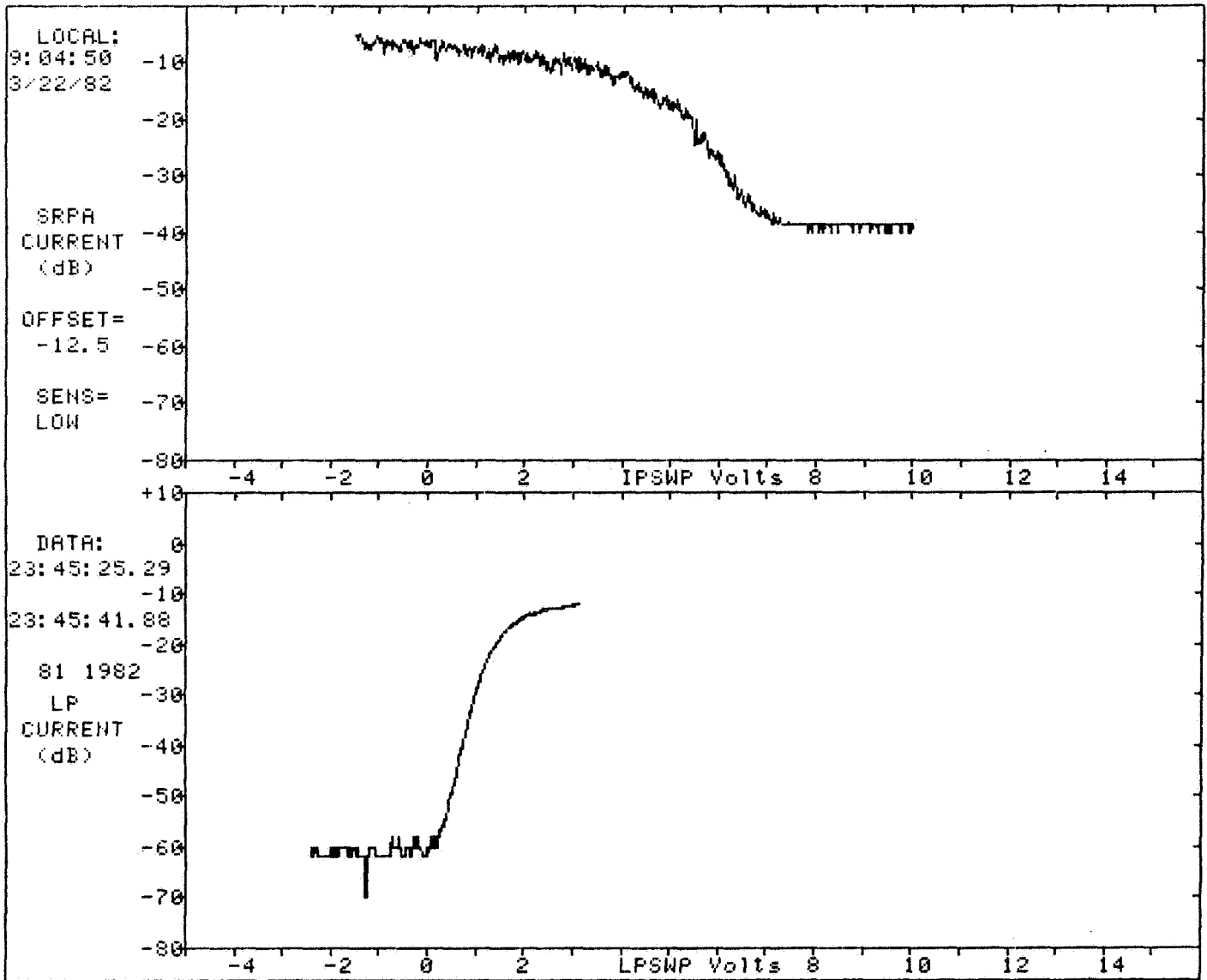


Figure 6. Location of the VCAP instrumentation on the OSS-1 pallet. The lower left in the figure was the forward side in the payload bay.

ORIGINAL PAGE IS
OF POOR QUALITY

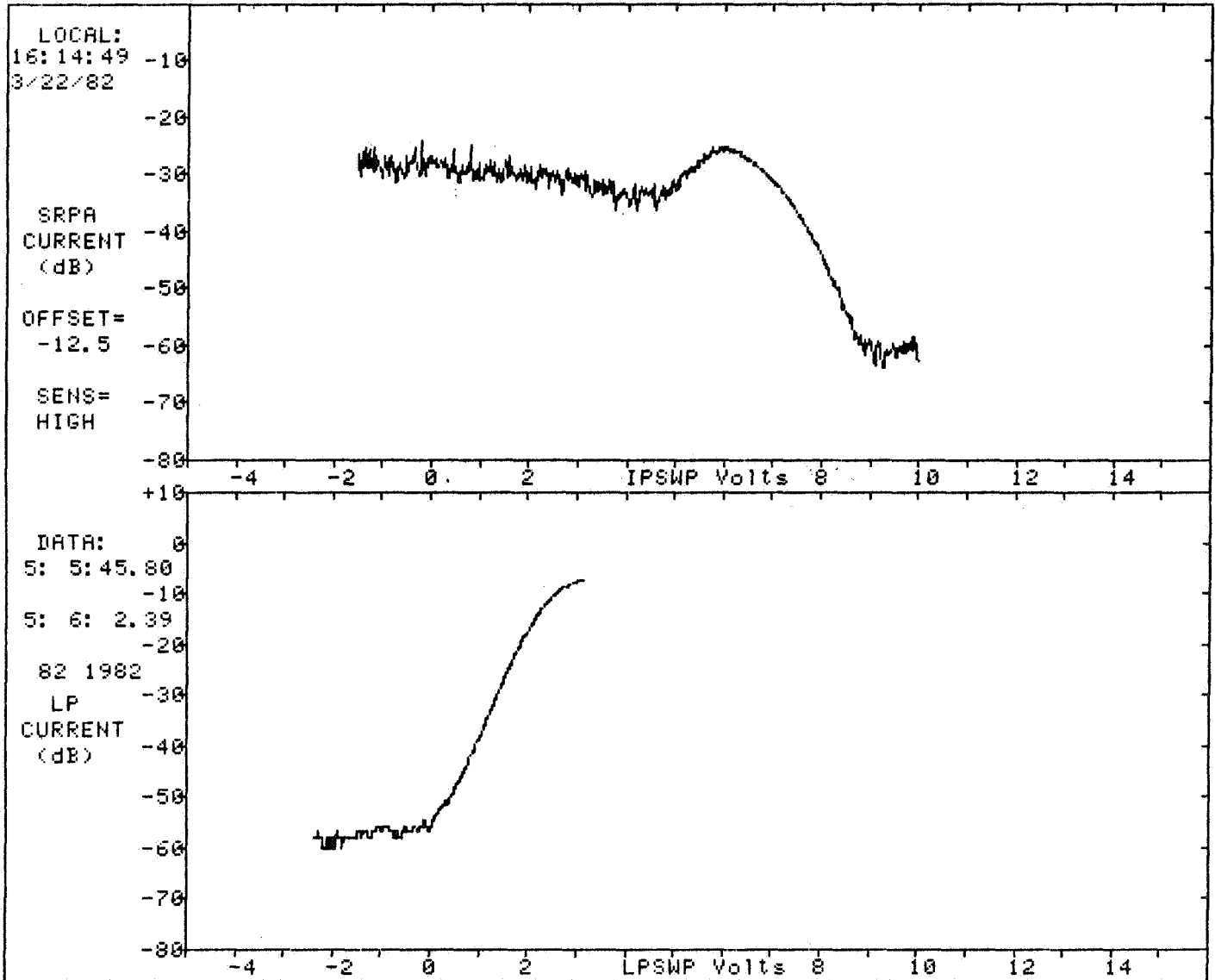
VEHICLE CHARGING AND POTENTIAL OSS-1/STS-3



DAY

Figure 7. Ion probe current (SRPA) and electron probe current (Langmuir probe) when the payload bay is in the ram direction in sunlight.

VEHICLE CHARGING AND POTENTIAL OSS-1/STS-3



NIGHT

Figure 8. Ion probe current (SRPA) and electron probe current (Langmuir probe) when the payload bay is in the ram direction and shadowed.

ORIGINAL PAGE IS
OF POOR QUALITY

VEHICLE CHARGING AND POTENTIAL OSS-1/ STS-3

LANGMUIR PROBE & SPHERICAL RETARDING POTENTIAL ANALYZER
34 SECOND AVERAGES

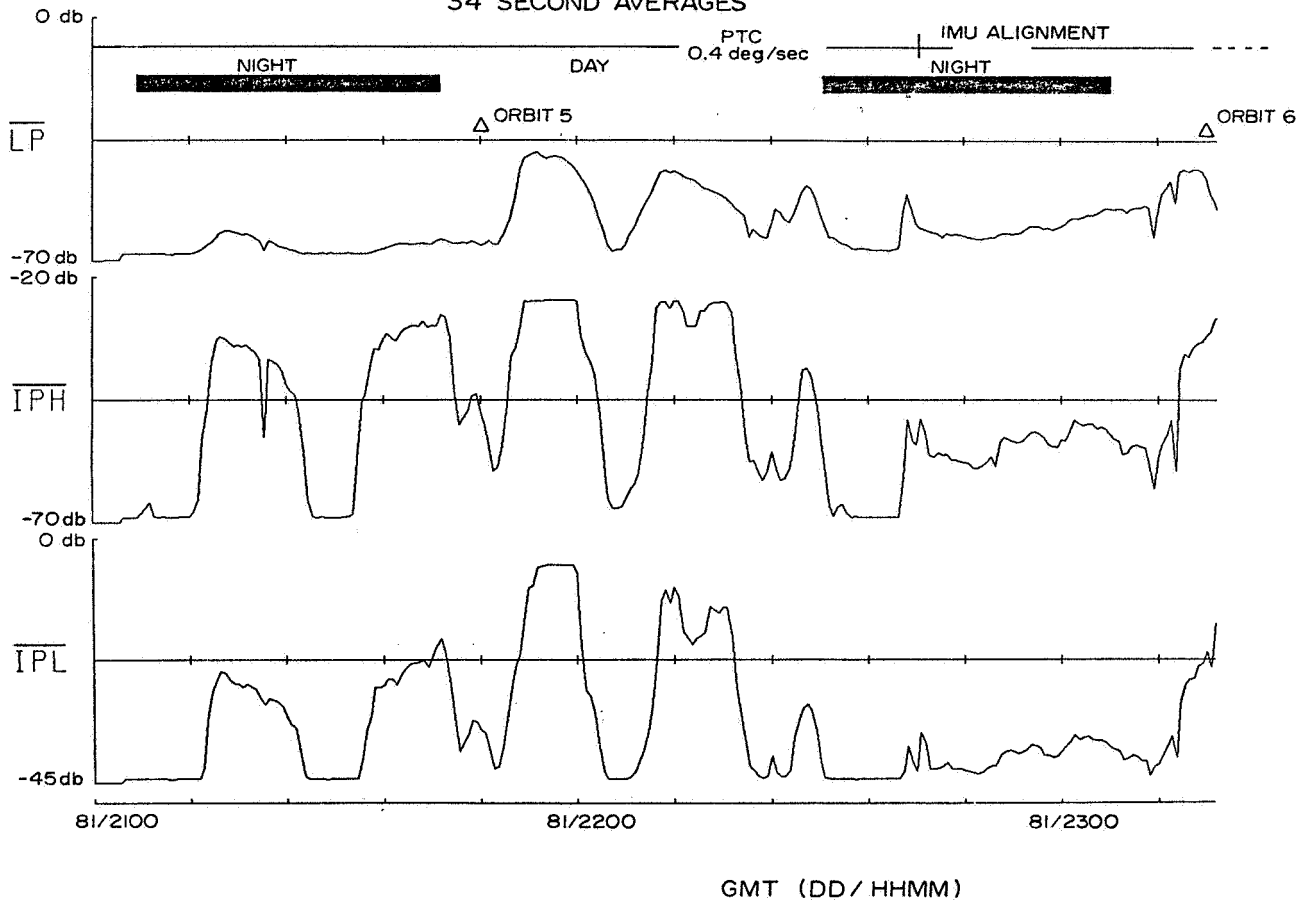


Figure 9. Langmuir probe current (LP), ion probe high range (IPH) and low range (IPL) current averaged over 34 seconds. The variations from near zero to maximum scale occur as the vehicle rolls with respect to the velocity vector and the payload bay alternately faces the ram and wake directions.

START GMT=82 /7 /29/19

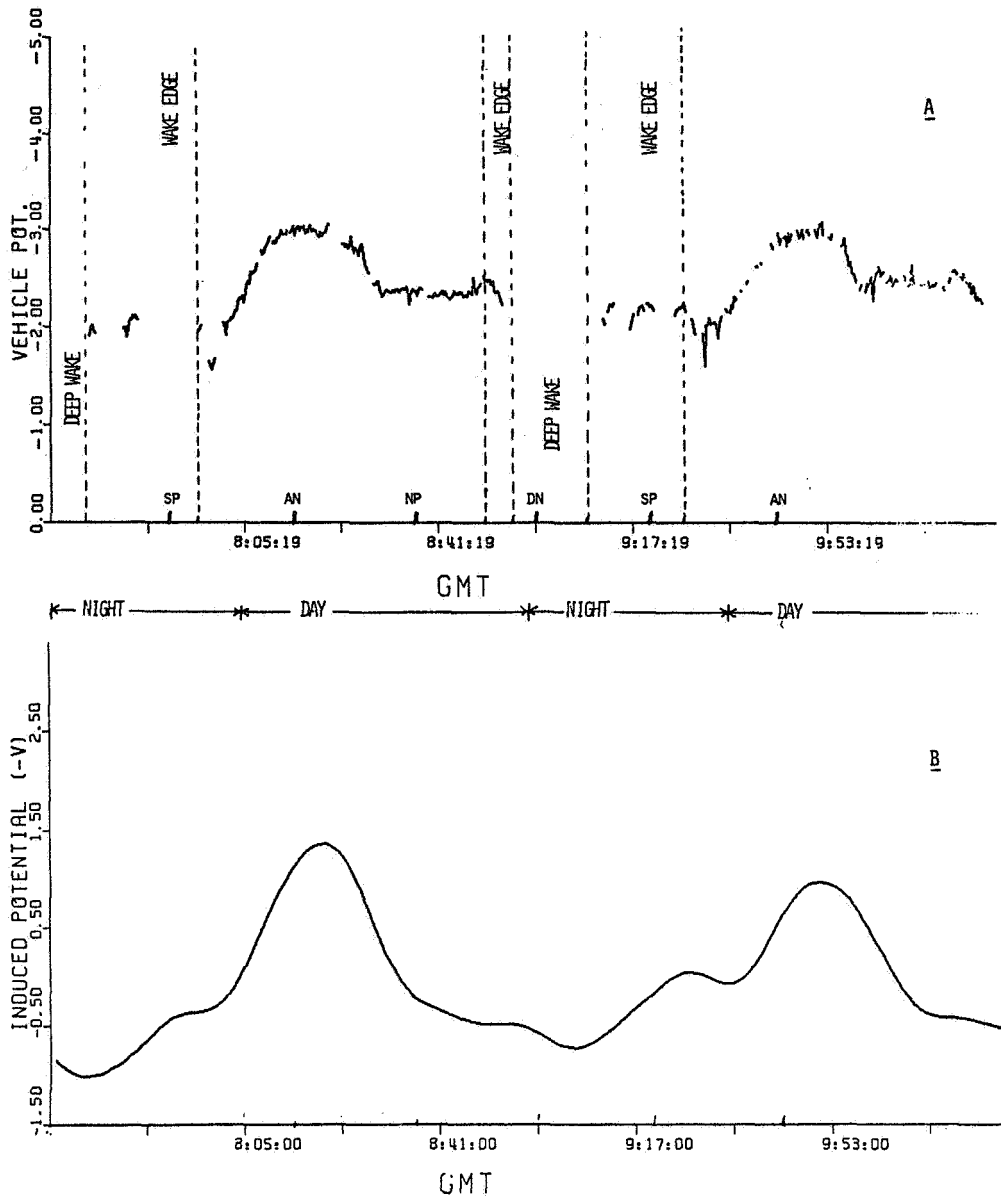
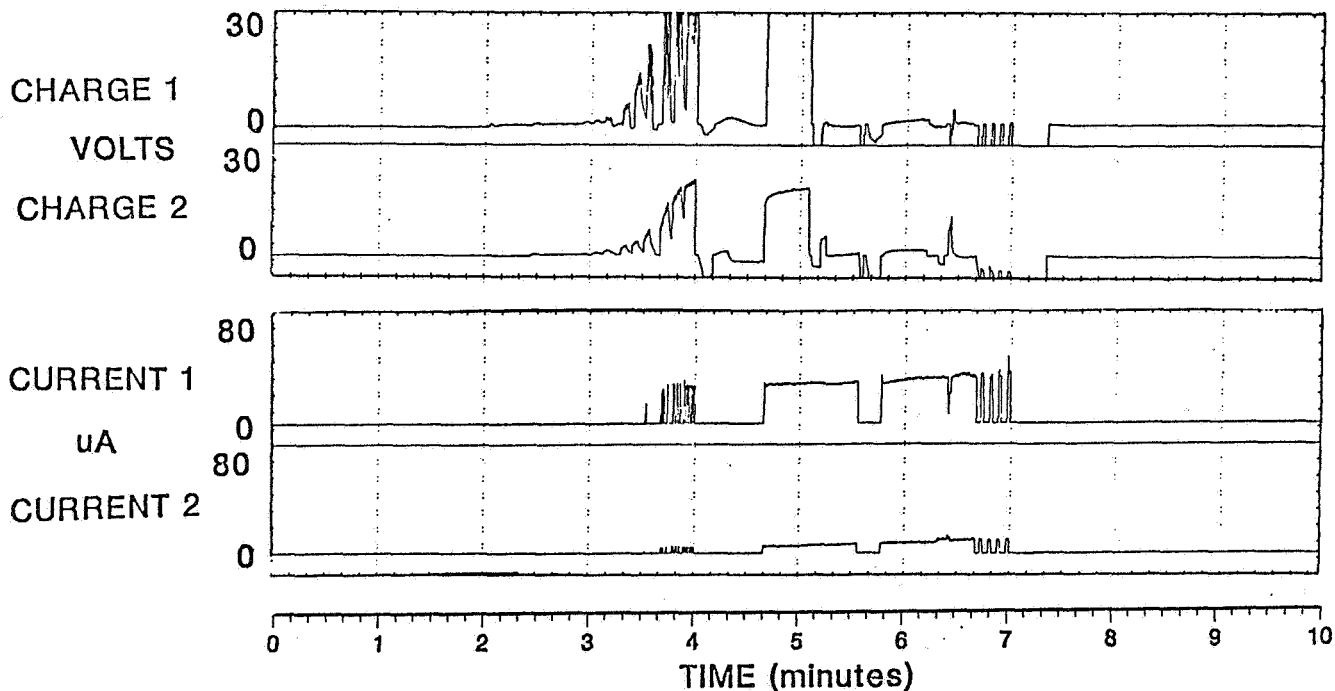


Figure 10. Vehicle potential at the location of the SRPA. The measured values are shown in Fig. 10A as determined by the offset potential of the Langmuir probe. The computed value of the potential is given in Fig. 10B assuming that the reference point is the main engine nozzles.

Vehicle Charging And Potential

VCAP SU/USU
OSS-1 STS-3 Launch March 22, 1982



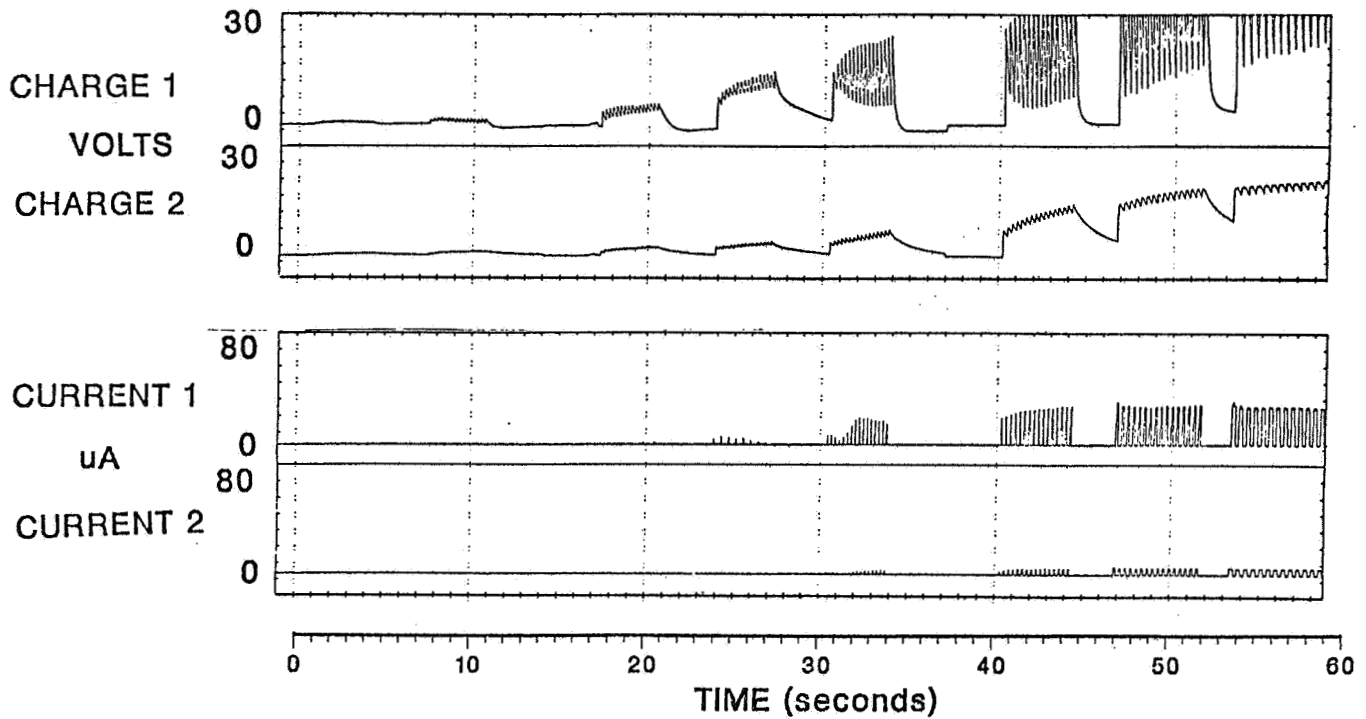
START TIME 84/ 0420:00 -- CC SEQUENCE - NIGHT

Figure 11. Charge and current probe measurements of dielectric charging and return currents during a series of electron gun pulses emitted during the Charge Current (CC) sequence. CCP1 (Charge 1 and Current 1) data were measured adjacent to the FPEG and CCP2 (Charge 2 and Current 2) data were taken on the far corner of the pallet.

ORIGINAL PAGE IS
OF POOR QUALITY

Vehicle Charging And Potential

VCAP SU/USU
OSS-1 STS-3 Launch March 22, 1982



START TIME 84/ 0423:00 -- CC SEQUENCE - NIGHT

Figure 12. High time resolution for one minute of data shown in Fig. 11.